communications earth & environment

Article

https://doi.org/10.1038/s43247-024-01326-6

Philippine Sea plate and surrounding magmatism reveal the Antarctic-Zealandia, Pacific, and Indian mantle domain boundaries

Check for updates

Shengping Qian[1,2] ✉, Jeremy Tsung-Jui Wu[3,4] & Jonny Wu[5,6] ✉

Delineation of geochemically distinct domains in Earth's mantle is essential for understanding large-scale mantle convective flow and dynamics. Previous studies identify possible long-lived (>60 million-year) mantle isotopic domains (i.e. Antarctic-Zealandia, Pacific and Indian) near the Philippine Sea and western Pacific. Here we compile published basalt geochemistry of the Philippine Sea and surroundings and add new Mo isotopic and water content data for Gagua Ridge lavas, northwestern Philippine Sea, to distinguish slab-derived components during subduction. The water content, trace element, and Mo-Sr-Nd isotope compositions of Gagua Ridge arc lavas suggest that slab fluids and sediment melts are responsible for element recycling to the arc. The Philippine Sea basalts show both Indian and Zealandia-Antarctic Pb isotopic signatures; restoration of the basalt locations within a plate reconstruction shows the far-travelled Philippine Sea traversed these mantle domains. We establish the Indian mantle domain eastern boundary at ~120°E under SE Asia and the Indian Ocean. The Antarctic-Zealandia mantle domain lies south of ~10°N within the SW Pacific and has mostly remained in oceanic realms since ~400 Ma with only limited continental material input.

The Philippine Sea plate (PSP) is one of the largest marginal sea plates in SE Asia and surrounding western Pacific (Fig. 1), where the growth of ephemeral marginal sea basins and extensive subduction has significantly consumed the oceanic lithosphere and associated tectonic record in the region[1–6] Although details of PSP plate tectonic history are debated[7–10], the PSP is formed of a mosaic of oceanic basins that were active at various times between the Cretaceous to the present (reviewed below). This is significant because very few other tectonic records exist in the region that span this time period[1–5,7–10]. Moreover, the PSP traveled across a significant swath of the western Pacific and moved >2000 km northwards from equatorial latitudes since the early Cenozoic, making it one of the furthest-traveled tectonic plates on Earth during Cenozoic times[11]. Thus, the PSP arguably provides one of the most significant regional spatiotemporal tectonic records back to Cretaceous times.

Here we investigate the magmatic and geochemical history of the PSP and surroundings to investigate global geochemical domains with implications for regional tectonics. We synthesize published basalt geochemistry (i.e. Pb isotopes) across an extensive region from SE Asia and the Western Pacific to the Southern Ocean. We present new PSP geochemistry including Mo isotopes and water contents from lava samples from one of the oldest parts of the PSP at the Gagua Ridge bathymetric high[12–14] (Fig. 1) to better constrain the recycling process of the subducted slab and associated petrogenesis for arc magmatism. We combine our results with published geochemical data from Early Cretaceous to recent PSP volcanic arcs (i.e. Kyushu-Palau Ridge, the western Mariana Arc; and the active Izu-Bonin Mariana arc) (Fig. 1) to characterize the PSP within regional SE Asian magmatic arcs. Our results reveal the far-traveled PSP traversed the Indian-Pacific mantle geochemical domain boundary during the Cenozoic, allowing us to delineate global geochemical domain boundaries with more clarity than previously recognized with implications for the origin and stability of long-term mantle heterogeneities in Earth history.

[1]Southern Marine Science and Engineering Guangdong Laboratory (Guangzhou), Guangzhou, China. [2]State Key Laboratory of Marine Geology, Tongji University, Shanghai, China. [3]Institute of Earth Sciences, Academia Sinica, Taipei, Taiwan. [4]Department of Geosciences, University of Arizona, Tucson, USA. [5]Department of Earth and Atmospheric Sciences, University of Houston, Texas, USA. [6]Present address: Department of Geological Science and Engineering, University of Nevada, Reno, USA. ✉e-mail: qianshengping@126.com; jonnywu@arizona.edu

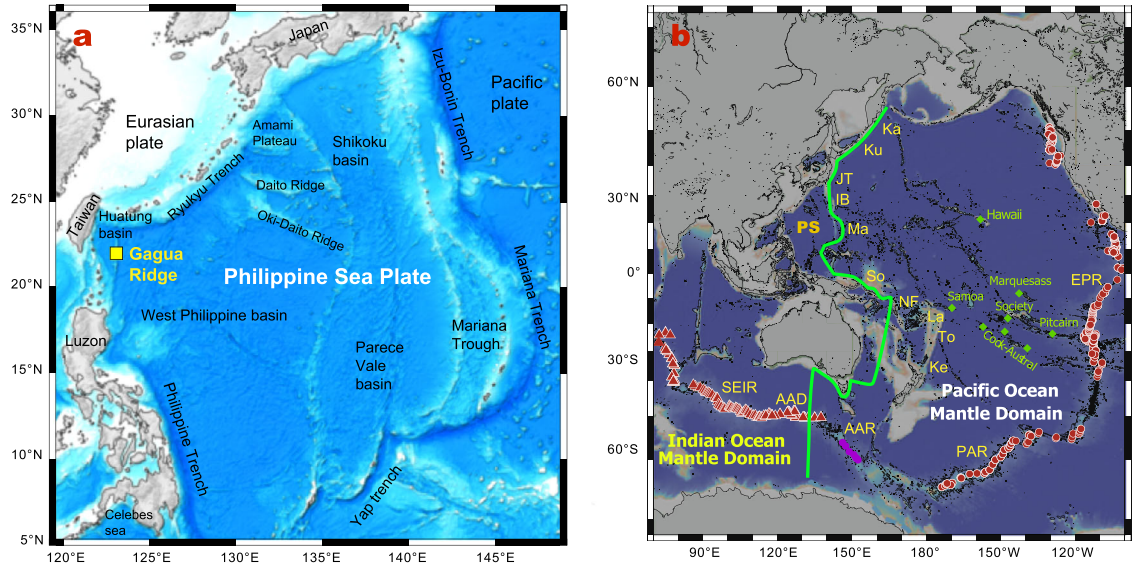

Fig. 1 | Sample locations and distribution of the Pacific and Indian Ocean mantle domains. a Geological map of the Philippine Sea plate and adjacent regions. The yellow square indicates the sampling location of Gagua Ridge lavas. **b** Distribution of the Pacific and Indian Ocean mantle domains. The bold green line depicts a proposed boundary between the Indian and Pacific Ocean mantle domains[28].

The Indian, Pacific, and Zealandia-Antarctic mantle domains

Delineation of geochemically distinct mantle domains and their secular distributions is essential for understanding both the pattern of large-scale mantle convection flow and the dynamics of the Earth's mantle. It is widely acknowledged that a distinct geochemical isotopic contrast exists between the Pacific and Indian mid-ocean ridge basalts[15–21]. The Indian-type mantle domain is characterized by higher $^{208}Pb/^{204}Pb$, $^{87}Sr/^{86}Sr$, and lower $^{143}Nd/^{144}Nd$ at a given $^{206}Pb/^{204}Pb$ compared to the Pacific-type mantle[16,18,22]. Also, the Indian-type mantle domain is distinguished by more radiogenic Hf isotopes at a given Nd isotopic composition compared to the Pacific-type mantle domain[19,23]. These contrasted isotopic signatures imply the presence of at least two chemically distinct, global-scale mantle domains, the so-called Pacific and Indian mantle domains (Fig. 1b)[17,19]. The distinct isotopic differences suggest the existence of two large-scale and long-term mantle domains with limited interactions[24,25] and raise the question of the precise location of the Indian-Pacific mantle domain boundary.

The precise boundary between the Pacific and Indian mantle domains is unclear but is thought to occur within our study area near the western Pacific subduction zones (Fig. 1b)[26,27] or along the north-south-trending Kurile-Japan-Izu and Marianas-Vitiaz-Tonga trenches and the Australia-Antarctic discordance (AAD) (Fig. 1b)[19,20,26,28,29]. The Indian-Pacific mantle boundary is thought to have been present since the Permian[29] or the Cretaceous[26]. Adding complexity, in their study of the Australian-Antarctic Ridge (AAR) between the AAD and the Pacific, Park et al.[30] identified an additional Zealandia–Antarctic mantle domain that was isotopically distinct from Pacific and Indian MORBs beneath the Southern Ocean (purple dots in Fig. 1b). However, the Zealandia–Antarctic domain northern boundary and its possible extension into the western Pacific region was not defined, nor whether there is a secular evolution of the isotopic boundary between the Pacific and Indian mantle domain. Most PSP plate reconstructions show the far-traveled and long-lived plate traversing at least some of the Indian-Pacific domain boundary (Fig. 1b), concurrent with seafloor spreading in the PSP ocean basins. Thus, the PSP magmatic record within its ocean basins presents a key opportunity to probe for evidence of underlying mantle domain boundaries.

A brief review of Philippine Sea plate tectonic history

The PSP is bounded by the Eurasia-Sundaland plates to the west, the Pacific plate to the east, and the Indo-Australian plates to the south (Fig. 1). The PSP is mainly composed of oceanic basins and island arc lithosphere with Early Cretaceous to recent ages[31]. Two active ocean basins within the PSP have been spreading since the mid-Cenozoic: the Mariana Trough and Ayu Trough (Fig. 1). Younger inactive ocean basins Shikoku Basin and Parece Vela Basin at the eastern PSP formed from ~30 Ma until ~15 Ma[32,33]. The older inactive West Philippine Basin began seafloor spreading in the early Cenozoic, either at 58 Ma[9], 55 Ma[31], or 52–51 Ma[2]. Spreading initiation was likely triggered by a mantle plume based on chains of age-progressive oceanic plateaus astride the spreading center that show ocean island basalt (OIB)–like lavas[2,34,35]. The plume that initiated West Philippine Basin spreading seafloor spreading may still be active today under the Manus Basin, SW Pacific[7]. The West Philippine basin is surrounded by several Early Cretaceous terranes that include the Gagua Ridge (123–124 Ma)[12] to the west, the Amami Plateau (115–117 Ma)[36] to the north, and the proto-Philippine arc (Kansi volcanics, 126–110 Ma)[37] to the southwest. The geochemical features (e.g., Pb–Sr enrichments and Nb-Ta depletions) of the volcanic rocks show that igneous activity at that time was of island arc affinity[12,36,37]. The Huatung basin at the northwest PSP is a far less-studied part of the plate; here, geological studies indicate a Cretaceous age for the Huatung basin[1,35,38–40]. The Gagua Ridge bathymetric high, where new Mo geochemistry and lava water contents are presented in this paper, is positioned within this enigmatic region in one of the oldest (i.e. Early Cretaceous)[12] parts of the PSP (Fig. 1). Many origins have been proposed for the Gagua Ridge that include an uplifted sliver of oceanic crust[13], a former intraoceanic fracture zone[14], or a relict subduction zone[12,41]. Thus, the Gagua Ridge provides rare and important constraints for tectonic reconstructions of the PSP and surrounding regions, where most of the Cretaceous-aged oceanic lithosphere has been subducted.

Results

Bulk rock and phenocryst compositions, Gagua Ridge, Philippine Sea

Molybdenum (Mo) is a fluid-mobile element in subduction systems, like Pb, B, and Ba, but this mobility is also strongly affected by the redox state based on experimental constraints[42,43]. Mo isotopic fractionation during dehydration and fluid flow in the slab results in heavier isotopic signatures in the fluid phase, while the deep residual subducted slab would be enriched in isotopically light Mo[44,45]. Thus, Mo isotopes provide a potential means for distinguishing different slab components involved in subduction zone processes. Mo isotopic compositions and Mo concentrations of the Gagua Ridge arc lavas are reported in Supplementary Data 1 together with relevant

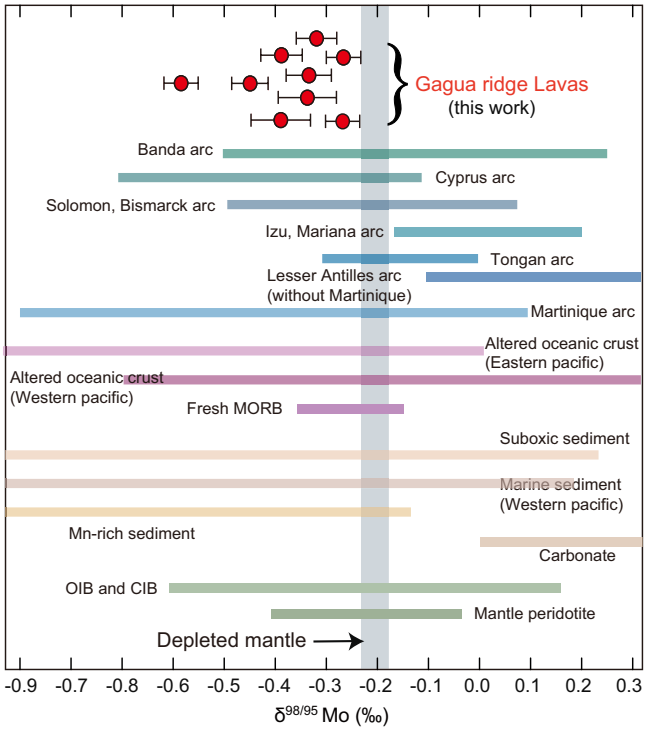

Fig. 2 | The Mo isotope compositions for the Gagua ridge lavas compared with other arc lavas, chondrite, mid-ocean ridge basalts, and sediment. Published Mo isotope data of lavas from Solomon, Bismarck and Cyprus arc[59]; Tongan arc[88]; Izu and Mariana arc[69]; Banda arc[61]; Martinique and Lesser Antilles arc[60,80]. Altered oceanic crust[45,88], and sediments[45,60,88], fresh MORBs[89,90], mantle peridotite, OIBs and continental intraplate basalts (CIB)[90] are also shown.

chemical and radiogenic isotope data on the same samples from our previous study[12] and additional data from this study. The $\delta^{98/95}$Mo values in the Gagua Ridge arc lavas span a considerable range, from −0.26 to −0.58 ‰ (Figs. 2; S3). Some Gagua Ridge arc lavas show lower $\delta^{98/95}$Mo values than MORB (Fig. 2). Compared to MORB, most Gagua Ridge arc lavas are substantially enriched in Mo over the similarly incompatible Ce (Fig. 3a). Samples from the Gagua Ridge arc have lower $\delta^{98/95}$Mo, Mo/Ce and Ba/Th ratios compared to the Mariana arc, which is also on the Philippine Sea plate (Fig. 3).

The cpx phenocrysts are diopsidic to augitic in composition, with Mg# values (Mg# = 100 × Mg / (Mg + Fe), mole %) from 72 to 83 (Supplementary Data 2). If the Fe–Mg exchange coefficient (K_d) is assumed to be 0.33 ± 0.03[46], the highest Mg# values of cpx phenocrysts in each sample are in equilibrium with the bulk-rock. Moreover, all the cpx phenocrysts (except two grains) have similar trace element characteristics with $(La/Yb)_N$ = 0.37–1.60, with an average 0.49 (Supplementary Data 3). The obtained H_2O contents of cpx phenocrysts are ranging from 138 to 811 ppm (Supplementary Data 2). The H_2O contents of melts in equilibrium with cpx phenocrysts are estimated according to the obtained cpx H_2O content, and the H_2O partition coefficients (D) between cpx phenocrysts and corresponding melt (equation (10)[47]. The calculated H_2O contents of the equilibrated melts yield a range from 1.18 to 7.09 wt.% (average 3.27 ± 1.32%) (Supplementary Data 2, Fig. S4). The H_2O/Ce ratios of the melts in equilibrium with the Gagua Ridge cpx generally exceed typical MORB (e.g., H_2O/Ce = 200 ± 100) but show similarities to global arc magma (Fig. 4).

Synthesis of published Pb isotopic compositions, western Pacific marginal basin and Southern Ocean lavas

Robust discriminants between the Indian and Pacific MORB source mantle domains (Fig. 5) include Δ 8/4, which is the magnitude of the $^{208}Pb/^{204}Pb$ divergence from a Northern Hemisphere basalt regression line[18], and Δ 7/6, the deviation of a given sample from a southern Pacific reference line defined as the best fit to the $^{207}Pb/^{206}Pb$–$^{208}Pb/^{206}Pb$ variations of the Pacific–Antarctic Ridge samples based on the least squares method[30]. The Australian-Antarctic Ridge (AAR) samples have Δ 8/4 of + 10 to + 18, which is higher than the samples from Pacific–Antarctic Ridge (−30 to +10) and East Pacific Rise (−10 to +10) but lower than the Indian ridge samples (greater than +22 and up to +80) (Fig. 5). The Δ 7/6 of AAR samples show negative values between –70 and –120, which is significantly lower than the Pacific–Antarctic Ridge samples (−10 and +10) (Fig. 5). Park et al.[30] demonstrated that the basalts from Australian–Antarctic Ridge have isotopic compositions distinct from both those from Pacific and Indian mantle domains, defining a separate Zealandia–Antarctic domain.

Using the criteria from ref. 30, we classify the Philippine Sea and regional ocean basin basalts into Pacific, Indian, and Zealandia-Antarctic domains using Δ 8/4 and Δ7/6 (Fig. 5). Surprisingly, in map view we find variable Pb isotopic signatures within the Philippine Sea plate itself (Figs. 5 and 6). The older (>34 Ma) and far-traveled West Philippine Sea basin basalts show Pb isotopic signatures similar to the Zealandia-Antarctic domain (purple dots in Fig. 6). In contrast, the adjacent, younger (<30 Ma) Shikoku and Parece Vela basins show Indian Ocean-type Pb isotopic signatures (orange dots in Fig. 6). The South China Sea, Celebes basin, and Sulu Sea basalts to the west of the Philippine Sea show Indian-type signatures whereas the areas near the Caroline Sea and Pacific show Zealandia-Antarctic signatures (Fig. 6).

Reconstruction of mantle domain locations

We utilized the Müller et al.[48] plate reconstruction model through pyGPlates to restore the basaltic rocks to their original eruption sites above the mantle source region. We also assigned mantle domains (i.e., Pacific, Indian, and Zealandia-Antarctic domains) to the basalts based on their initial Pb isotopic composition (Fig. 6). By integrating the paleo-locations with the designated mantle domains of the basalts, we developed a reconstructed mantle domain map in the SW Pacific region (Fig. 7). For the Zealandia-Antarctic domain, our reconstruction extends the domain boundary northwards to 10 °N latitude (red line in Fig. 7b). The previous boundary for the Zealandia-Antarctic domain introduced in ref. 30 (blue line in Fig. 7b) was restricted to very far south Southern Ocean regions (i.e. south of 40°S latitudes) and included only a definition of its southern, western and eastern limits.

The reconstructed Pb isotope signatures distinguish the far-traveled PSP from its surrounding ocean basins (Fig. 7b). The Manus basin, Fiji basin, and Lau basin basalts show Indian Ocean-type Pb isotopic signatures similar to the younger Shikoku-Parece Vela basins of the Philippine Sea (Figs. 7a; S6). Towards the south, the volcanic rocks from the Woodlark basin, Norfolk basin, Tasman Sea, New Zealand, and the South Ocean between East Australia and Antarctica show distinctive Pb isotope characteristics of the Zealandia-Antarctic mantle domain (Fig. 7).

Broadly, Indian domain signatures are seen east 130°E longitudes and Pacific signatures are seen west of ~180° longitude; the region between 130°E to 180° that includes the Philippine Sea plate shows a mixture of Zealandia-Antarctic and Indian signatures (Fig. 7a). The region with mixed signatures (i.e. between 130°E to 180°) include several mobile ocean basins that have diverse proposed plate reconstruction solutions; therefore, some uncertainty (±5 to 10° latitude and longitude) should be considered for the reconstructed sample locations. On the other hand, our results are generally reproduced when reconstructed in alternative Philippine Sea and East Asian plate models[6,49,50] (Fig. S7).

Discussion

Insights on Gagua Ridge magmatic history

The calculated H_2O contents of the Gagua Ridge equilibrated melts with the cpx phenocrysts (within 40% uncertainty; see Methods) span a wide range, from 1.18 to 7.09 wt.% (ave. 3.27 ± 1.32%), with most being higher than 2 wt.% (Fig. S4). In addition, the H_2O contents of the equilibrium melts do not correlate with the Mg# of the cpx (Fig. S4). This suggests that the H_2O

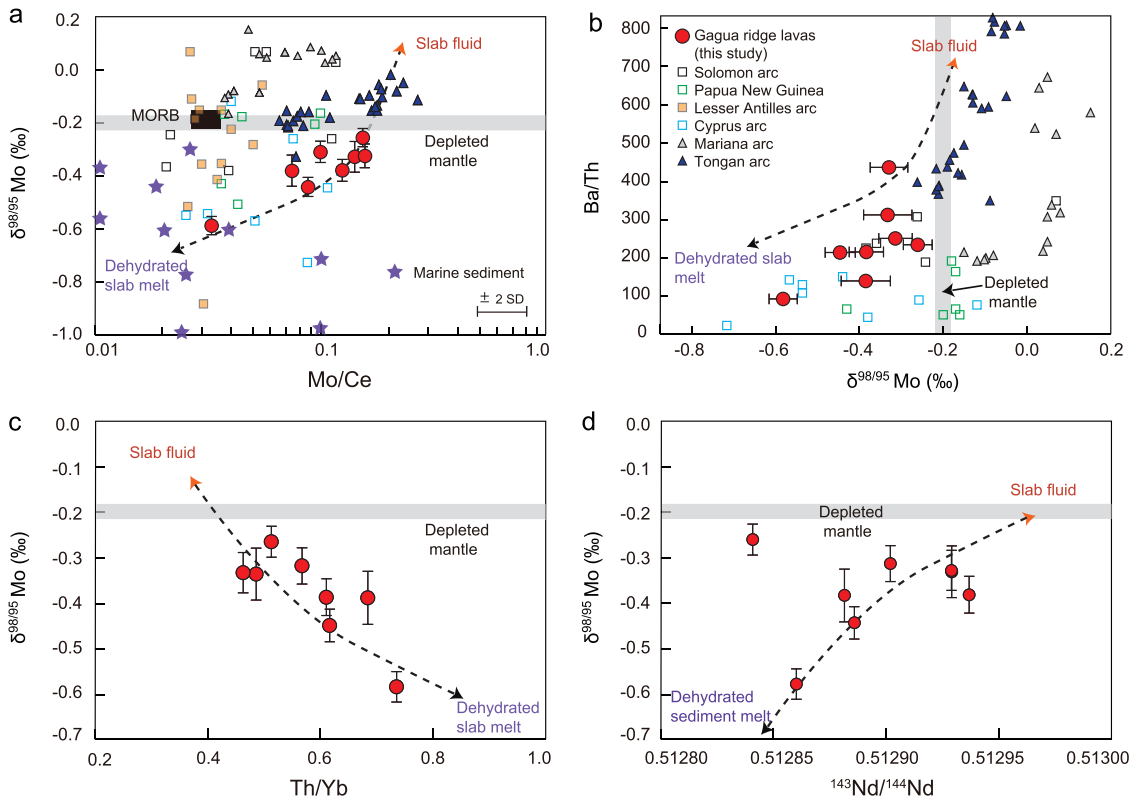

Fig. 3 | Mo and Nd isotope and trace element systematics of Gagua ridge lavas. a $\delta^{98/95}$Mo vs. Mo/Ce plot. **b** Ba/Th vs. $^{98/95}$Mo plot. **c** $^{98/95}$Mo vs. Th/Yb plot. **d** $^{98/95}$Mo vs. ^{143}Nd/^{143}Nd plot. Data sources for arc lavas, sediments, and MORBs as in Fig. 2. Depleted mantle values from ref. 89, 91. Trace element and Mo isotope ratios of sediments are from ref. 45, 51.

content in the magmatic system remained almost constant during magma evolution. In order to minimize the possible effects of fractionation, we select only Cpx with Mg# > 75 to calculate the water content of the equilibrium melts. We find the calculated water content of the Gagua Ridge arc melts in equilibrium with the cpx varies from 1.18 to 7.09 wt.%. Despite uncertainties of up to 40%, these water contents are apparently higher than those of MORB, OIB and back-arc basin basalts (BABB, 0.2–2.0 wt.%) but fall within the range of global island arc lavas (Fig. S4, 2.0–8.0 wt.%)[51,52]. Owing to the similar incompatibility in minerals between H_2O and Ce[53], it is generally believed that the H_2O/Ce ratio is independent of both fractionation and degree of mantle melting and represents that of the mantle source. The H_2O/Ce ratios of the Gagua Ridge lavas significantly exceed the range of typical lavas at mid-ocean ridges and ocean islands (e.g., H_2O/Ce = 200 ± 100)[53,54] and are similar to the range of typical island arc lavas (Fig. 4). Thus, our characterization of Gagua Ridge lava volatiles strengthens the evidence that the Gagua Ridge represents a remnant volcanic island arc[12].

The candidate slab-derived components to the mantle source during subduction are complex, including hydrous melts, aqueous fluids, and supercritical liquids originating from altered oceanic crust, subducted sediments, and the underlying lithospheric mantle[55–58]. We now review the possible contribution of different slab-derived components to the mantle source based on the trace element, and Mo and other isotopic compositions of Gagua Ridge lavas. $\delta^{98/95}$Mo of Gagua Ridge arc lavas show relatively good covariation with Ba/Th and Mo/Ce (Fig. 3), indicating that at least two geochemical reservoirs (one with heavy Mo isotopes and a second with light Mo isotopic signatures) were involved in the generation of Gagua Ridge lavas. Generally, it is believed that LILE (e.g., Mo, Ba, and Sr) can be easily transported by slab-derived fluid[51,57]. For instance, the increasing role of slab fluids may be inferred from the enrichment of fluid-mobile Mo over the similarly incompatible Ce, and increasing Ba/Th in most Mariana and Tonga arc magmas[45,59]. The high $\delta^{98/95}$Mo, Mo/Ce and Ba/Th signatures in Gagua Ridge arc lavas, similar to Mariana and Tongan arc lavas, largely reflect aqueous fluid contributions from the slab, as slab dehydration can efficiently fractionate the ratio between a fluid-mobile element and an immobile element (e.g. Ba/Th, Ce/Mo) (Fig. 3). The isotopically heavy ^{98}Mo is preferentially released into the fluid phase during subduction slab dehydration, while the residual slab would be expected to retain isotopically lighter Mo[45,59–61]. Thus, the isotopically heavy Mo signatures of some Gagua Ridge lavas are likely inherited from subducted slab-derived fluids.

The origin of isotopically light Mo signatures of global arc lavas has remained enigmatic. One possibility has been suggested is that partial melting of residual slab after slab dehydration might have delivered isotopically light Mo and low Mo/Ce to the depleted sub-arc mantle[44]. Notably, the Gagua Ridge lavas with isotopically lighter $\delta^{98/95}$Mo have less radiogenic ^{143}Nd/^{144}Nd (Fig. 3d). This implies that the depleted MORB eclogites cannot be the possible candidate, as the enriched component (isotopically light Mo) with less radiogenic Nd isotopes are required. Alternatively, the breakdown of secondary minerals during subducted sediment melting might have delivered isotopically light Mo to the depleted sub-arc mantle[59]. Some pelagic sediments, especially radiolarite/claystones from Mariana, show a very light Mo isotope composition[45,60] (Fig. 3). However, the Gagua arc lavas and other arc lavas with light Mo isotope signatures (Fig. 3) also show relatively low Mo/Ce, suggesting that the subducted material already lost Mo prior to slab melting[59,62,63]; this is difficult to explain via a simple aqueous fluid or melt addition from the subducted sediment. The residual subducted sediment after dehydration would be expected to have relatively low Mo/Ce. As the slab becomes progressively more dehydrated, it becomes isotopically lighter as Mo-enriched fluids are removed. Moreover, the variations of Th/Yb of the Gagua Ridge lavas (Fig. 3) also underline a significant contribution of subducted sediment to the mantle source. Thus, a multi-stage metasomatism of the sub-arc mantle is proposed to be responsible for the recycling of Mo and possibly other elements. Our data document fluid-related Mo loss upon an early subduction stage and preferential incorporation of heavy

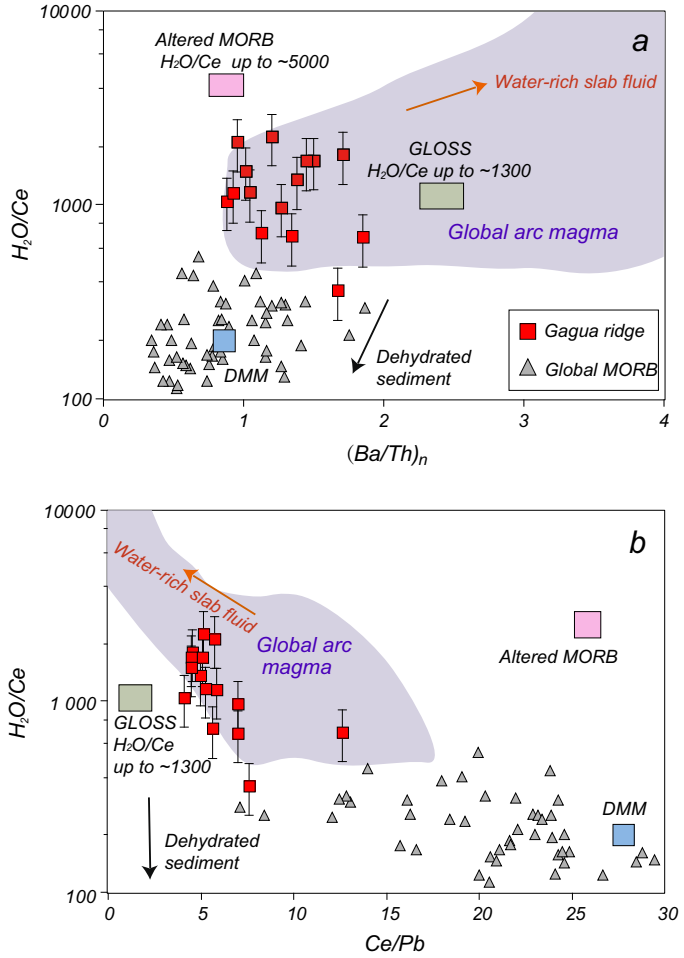

Fig. 4 | Comparison of the water contents with other trace element concentrations in clinopyroxene in this study. a Comparison of H_2O/Ce with Ba/Th, (**b**) H_2O/Ce versus Ce/Pb plot. Data from global arc lavas are included for comparison[92]. The H_2O/Ce and Ba/Th ratios of DMM, GLOSS, altered upper oceanic crust are from ref. 51, 53, 54, 91. The H_2O/Ce ratios of the dehydrated sediment are from ref. 53; the ratios of Ba/Th of dehydrated sediment are calculated based on the data from ref. 51 and the mobility from ref. 93.

Mo into the sub-arc mantle, which can account for observed high Mo/Ce and $\delta^{98/95}$Mo in some lavas compared to the mantle. Subsequently, partial melting of subducted residual sediment can explain relatively low Mo/Ce (and Ba/Th), high Th/Yb, and extremely low $\delta^{98/95}$Mo observed in our samples, and Lesser Antilles, Papua New Guinea, and Cyprus arc lavas. In summary, considering both the analyses of water contents and other geochemical features of the Gagua Ridge lavas, it seems that their mantle source was metasomatized by subduction-related fluids and melts originating from oceanic crust and sediments.

Philippine Sea plate tectonic implications

The large-ion lithophile element Pb is highly mobile during slab dehydration or melting, and the origin of Pb in arc lavas is often evaluated by combining the isotopes with fluid-mobile and -immobile elements ratios (such as Nd/Pb)[27,64]. As shown in Fig. 8, the Gagua Ridge lavas show a typical arc 'fluid' signature with high Pb concentrations (4.5–6.8 ppm) and low Nd/Pb < 5 (relative to MORBs ~20–25[65]). The percentage of Pb derived from the subducting slab for the arc lavas can be estimated following the methods of Pearce et al.[66]. The results show that a very high ~90 ± 7% of the Gagua Ridge arc, Amami Plateau, and proto-Philippine arc Pb is derived from the subducting slab (Fig. 8a). Our new water contents, Mo isotope, and other trace element features of the Gagua Ridge lavas similarly show a significant contribution of subducted slabs (including sediments and oceanic crust) to the sub-arc mantle (Figs. 4 and 8). Furthermore, as shown in Fig. 8b, most arc lavas (e.g., Gagua Ridge arc, Amami Plateau, proto-Philippine arc, and Mariana arc) display an overall, near-vertical trend on the $^{204}Pb/^{206}Pb$-Nd/Pb crossplot, which supports the mixing of radiogenic and unradiogenic slab-derived Pb, but not slab–mantle mixing. Overall, this evidence indicates that most of the Pb and Pb isotopes of the Gagua Ridge arc, Amami Plateau, and proto-Philippine arc are largely controlled by slab inputs. In other words, the Pb isotope trend most likely indicates binary mixing of two important slab components: subducting MORB and sediment. The subducting sediment is clearly implicated as the radiogenic endmember, while the subducting oceanic crust (MORB) is a likely source for the unradiogenic endmember (Fig. 8b, c).

The Gagua Ridge arc lavas have lower Δ8/4 values that resemble Tonga–Kermadec and Mariana arc lavas; at these locations, Pacific MORB has subducted beneath another oceanic plate. Conversely, the Gagua Ridge lavas are remarkably different from the Luzon, Ryukyu, and Honshu arc samples with higher Δ8/4 (Fig. 8c) where Indian-type MORB is subducting. Thus, the low Δ8/4 signal (Δ8/4 < 40) of the Gagua Ridge identifies the subducting MORB crust as Pacific-type (Fig. 8c). Ar-Ar dating indicates the Gagua Ridge lavas were formed in the early Cretaceous (~123–124 Ma)[12]. Thus, it is most likely that the Gagua Ridge lavas are derived from a mantle source region metasomatised by slab-derived materials with Pacific Ocean-type MORB Pb isotopes. Comparison to Nd/Pb and Pb isotopes of surrounding Early Cretaceous arc rocks from the Amami Plateau in northern West Philippine Basin, 126–110 Ma Kansi volcanics along proto-Philippine arc, and Early Cenozoic Izu–Bonin arc magmatism (>42 Ma) show similarities to the Gagua Ridge lavas, suggesting that the subduction components in the source were generated from subducting Pacific Ocean-type oceanic crust (Fig. 8a).

In contrast, the West Philippine basin lavas within the PSP show MORB-OIB-like trace element characteristics rather than island arc characteristics[67]. Compared to the West Philippine basin lavas, the Shikoku and Parece Vela basins of the PSP, and Celebes and Sulu Sea are typical back-arcs and more likely affected by slab subduction during the basin development. As shown in Fig. S5, the Nd/Pb and Pb isotopes of Shikoku and Parece Vela basins, and Celebes and the Sulu Sea are back-arc basin-like magmas (e.g. Mariana Trough), which are largely interpreted by slab and mantle mixing trends. Thus, the geochemical compositions of the lavas with relatively high Nd/Pb (>15) are selected to reflect their sub-arc mantle source.

In terms of Pb isotopes, magmatism within the PSP from the older West Philippine basin shows Zealandia-Antarctic domain signatures whereas the younger Shikoku and Parece Vela basins show Indian domain magmatic signatures (Figs. 5–7). Although this magmatic history could be explained by a heterogenous mantle or a transient mantle source over time, the simplest explanation is that the far-traveled and fast-moving Philippine Sea plate moved across a mantle domain boundary during its northward journey. The anomalous Zealandia-Antarctic magmatism within the West Philippine Basin that is now sandwiched between Indian domain magmatism within SE Asia (i.e., South China Sea, Sulu Sea, Celebes Sea) and the Shikoku-Parece Vela basins (Figs. 6 and 7a). However, when the West Philippine basin magmatism is palinspastically-restored within a plate reconstruction (Fig. 9), the Pb isotopic signatures fits with other Zealandia-Antarctic magmatic signatures to the south (Fig. 7b), and the apparent Pb isotope misfit with its present surroundings is reconciled.

One important implication of our reconstruction is for the debated origin of the Celebes Sea within SE Asia (Fig. 6). Previously, it has been proposed that the West Philippine basin and Celebes Sea basin were interconnected during the middle Eocene (50–37 Ma) based on similar seafloor spreading timings and paleolatitudes in a plate reconstruction[68]. However, the Celebes Sea basin (43 Ma) lavas exhibit Pb isotopic signatures different from the Zealandia-Antarctic ridge and seamount and west Philippine basin lavas but show coherent relationships with the Indian MORBs (Figs. 5, 6 and S5). Therefore, the proposed West Philippine Basin-Celebes Sea connection is not supported here; the Pb isotopes and trace element

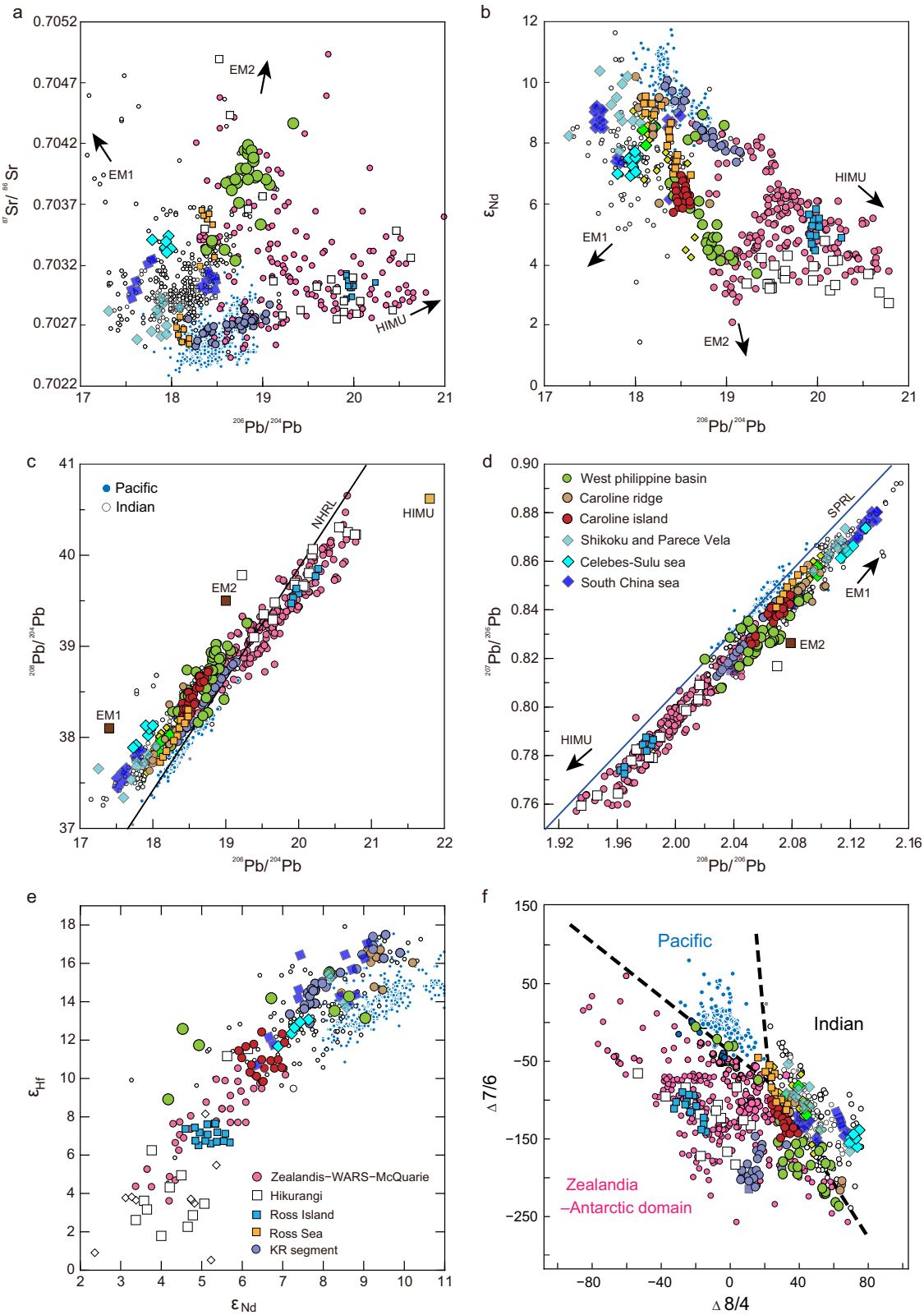

Fig. 5 | Oceanic mantle domain areas shown by comparisons between isotope ratios from the Philippine Sea plate, other mid-ocean ridge segments, and surrounding regions. a Plot of $^{87}Sr/^{86}Sr$ versus $^{206}Pb/^{204}Pb$. **b** εNd versus $^{206}Pb/^{204}Pb$. **c** $^{208}Pb/^{204}Pb$ versus $^{206}Pb/^{204}Pb$. **d** $^{207}Pb/^{206}Pb$ versus $^{208}Pb/^{206}Pb$. **e** εHf versus εNd. **f** Clear separations between the Pacific MORB, Indian MORB, and Zealandia domain lavas are evident. The West Philippine basin, Caroline basin, Ross Island, Hikurangi Plateau, and Zealandia have similar isotope features and show strong similarities with EM2/HIMU–type mantle reservoirs as demonstrated by the relatively radiogenic $^{206}Pb/^{204}Pb$ and $^{208}Pb/^{204}Pb$. In contrast, the isotope ratios of the lavas from east Philippine basin, South China Sea, Manus basin, Fiji basin, Lau basin, Woodlark basin, and Southern Sea reflect compositions closer to the EM1 end-member due to lower $^{206}Pb/^{204}Pb$ (higher $^{207}Pb/^{206}Pb$ and $^{208}Pb/^{206}Pb$). The West Philippine basin, Caroline basin, Ross Island, Marie Byrd, and Zealandia data plot below the SPRL[30] and are distinct from Indian and Pacific signatures. The NHRL is based on ref. 18. EM1, enriched mantle 1; EM2, enriched mantle 2; HIMU, high-μ ($^{238}U/^{204}Pb$). The MORB data are mostly from ref. 94 and references therein; Pb isotope data of the Australia-Zealandia domain from ref. 30, the geochemical data on west Pacific marginal basin were from the GEOROC database[85].

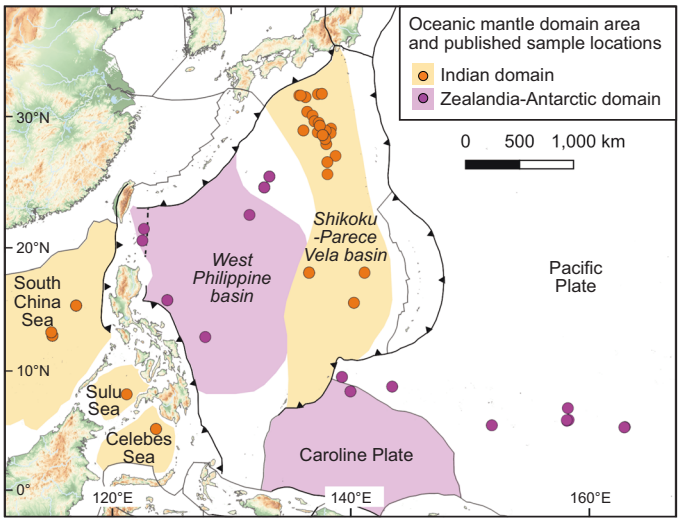

Fig. 6 | Mantle domains of the Philippine Sea plate and surroundings. The mantle domains are constrained by Pb isotopic compositions of basalts (circles) that are color-coded orange for the Indian domain and purple for the Zealandia-Antarctic domain.

features (Figs. 5, S5) of West Philippine Basin lavas are clearly different from those of Celebes Sea basin lavas.

Implications for geochemical domain boundaries and regional SE Asian tectonics

The Indian, Pacific, and Zealandia-Antarctic domains are among the most prominent mantle chemical heterogeneity zones on Earth but their locations are not fully delineated[26,30]. We reconstruct our analyzed Pb isotope locations within a plate reconstruction[48] and newly show the Zealandia-Antarctic domain lies under the SW Pacific roughly between longitudes 100°E and 160°W and south of ~10°N (i.e., mostly within the southern hemisphere) (red line in Fig. 7b). Our new mapping extends the Zealandia-Antarctic boundary of ref. 30 significantly northwards by about 40° latitude whereas the longitudinal extent is unchanged (compare red and blue lines in Fig. 7b). Using our northern boundary, the size of the Zealandia-Antarctic domain could be three times larger than previously recognized (~51 × 10^6 km^2 compared to ~16 × 10^6 km^2; Fig. 7b). This larger size is conceivable given that Park et al.[30] speculated the Zealandia-Antarctic domain boundary was potentially sourced by deep mantle upwellings that mixed with the upper mantle. A mixed shallow-deep mantle source seems possible because the northern reaches of our newly delineated Zealandia-Antarctic domain straddles a major zone of imaged, plume-like tomographic anomalies within the central Pacific[69] where some studies indicate plumes of shallower origin (i.e., base of transition zone)[70]. We cannot precisely constrain the Zealandia-Antarctic domain western boundary under Australia due to possible geochemical contamination from Australian continental crust nor the eastern domain boundary due to sparse data (see dashed red lines in Fig. 7b).

The most northerly sites that show Zealandia-Antarctic domain signatures are presently located around 20°N within the West Philippine basin, PSP (Figs. 6 and 7a); however, when reconstructed these locations shift southwards near the equator or further south (Fig. 7b). This pattern is consistent with PSP paleomagnetism that indicates the plate originated near the equator and translated 2000 km northwards since the Eocene[11] (Fig. 9). Indeed, the magmatism from the older portions of the PSP (i.e., the west Philippine basin) show Zealandia-Antarctic domain signatures that are more similar to areas to the south within the SW Pacific (i.e., Caroline Sea, Woodlark basin, Norfolk basin, Tasman Sea, New Zealand, Hikurangi oceanic plateau, and the Southern Ocean between East Australia and Antarctica) than the areas surrounding the present PSP (Figs. 5–7a).

Sites within the Indian Ocean and most of SE Asia (i.e., South China Sea, Celebes basin, Sulu basin, Shikoku and Parece Vela back-arc basin, Fiji basin, and Lau basin) within our analyzed age range of 95 to 0 Ma show Indian domain signatures (Figs. 6 and 7a). These sites establish the eastern Indian domain boundary under SE Asia and under the Indian Ocean west of ~120°E. Pacific domain rocks (green dots in Fig. 7) are primarily from the present Pacific-Antarctic ridge and East Pacific Rise, with some younger 5 to 0 Ma rocks in the Woodlark basin also showing Pacific domain signatures (Fig. 7). Notably, the Caroline ridge, Ross Sea and Macquarie Ridge plot on the boundary between Indian domain and Zealandia-Antarctic domain, whereas volcanic rocks from the Caroline Islands and Ross Island lavas with OIB-like signatures that are related to plumes[71,72] show a Zealandia-mantle signature (Fig. 5). Similarly, the Hikurangi oceanic plateau and West Philippine lavas (i.e. Benham rise) related to plumes show Zealandia-mantle signature[2,73] (Fig. 5). Thus, the ocean islands and plateau affected by hotspots show more obvious Zealandia-Antarctic domain signatures and we infer the Zealandia-Antarctic mantle domain has been affected by the deep mantle. This inference supports previous studies that the magmatism of Zealandia, the Hikurangi Plateau, and surrounding area[73–76] shows mixing of a deep mantle upwelling with a heterogeneous upper mantle. Volcanic isotope geochemistry allows us to distinguish a greater contribution from a high-μ (HIMU)/EM2 reservoir in the Zealandia mantle domain areas relative to a more strongly EM1-like reservoir in the Indian mantle domain areas (Fig. 5). Again, this would reflect a greater influence of deep mantle plume influx beneath the Zealandia region.

Secular evolution of the geochemical domains

The stability of upper mantle heterogeneity domains remains controversial. While several geological processes can modify isotopic mantle domains, such as subduction[77] and deep mantle plume contamination[78], others also suggested that domain boundaries are relatively stable within a minimum hundred-million-year timescale[29]. Our constraints are mainly from Cenozoic basalts (1247 of 1281 samples); thus, we can show that our newly defined Zealandia-Antarctic domain boundary with the Pacific and Indian domains has likely remained relatively stable since at least 56 Ma.

To go back further in time, we examine our new Zealandia-Antarctic domain boundary (red line in Fig. 7b) within a 400 to 0 Ma tectonic plate reconstruction model (Supplementary Movie 1) over a time period that roughly covers the most recent supercontinent cycle. We integrate our domain boundaries with published localities of deep mantle plumes[79] fixed to a mantle reference[48] and test the possibility of stable, longer-term (100's of Myr) mantle domain boundaries since 400 Ma. Our resulting reconstruction movie (Supplementary Movie 1) reveals that our mapped Zealandia-Antarctic domain has mostly remained within oceanic realms since ~400 Ma. In addition, deep mantle plume activities in the area are mostly away from the central part of the Zealandia-Antarctic domain but located to the north and east within the Pacific realm. Therefore, we suggest the Zealandia-Antarctic domain may have some input from mantle plumes but only limited modification from continental input, which would show contrasted and obvious geochemical signatures. On the contrary, recent plate reconstructions for the western Pacific-Panthalassa imply multiple intra-oceanic subduction zones in the area[6]. Therefore, the Zealandia-Antarctic domain is likely to have accumulated input from mantle plumes and subducted oceanic lithosphere during its history, since at least 400 Ma. Put simply, throughout this protracted period since 400 Ma, the Zealandia-Antarctic domain has largely remained free from tectonic interactions with continents, thereby distinguishing it as a geochemical enclave that is relatively devoid of subducted continental material.

Methods

Whole-rock Mo isotopes

Lavas from the Gagua Ridge were collected by ROV during the Haixing6000 first sea trial in October 2018 (Fig. S1). All Gagua Ridge lavas are relatively fresh andesites that are massive and porphyritic, containing clinopyroxene, orthopyroxene and plagioclase, together with minor apatite and Fe-Ti oxides, as phenocrysts, while the sub-oriented fine-grained plagioclases and pyroxenes are preserved in the groundmass exhibiting hyalopilitic texture (Fig. S2). After the removal of weathered or altered surfaces, the fresh parts

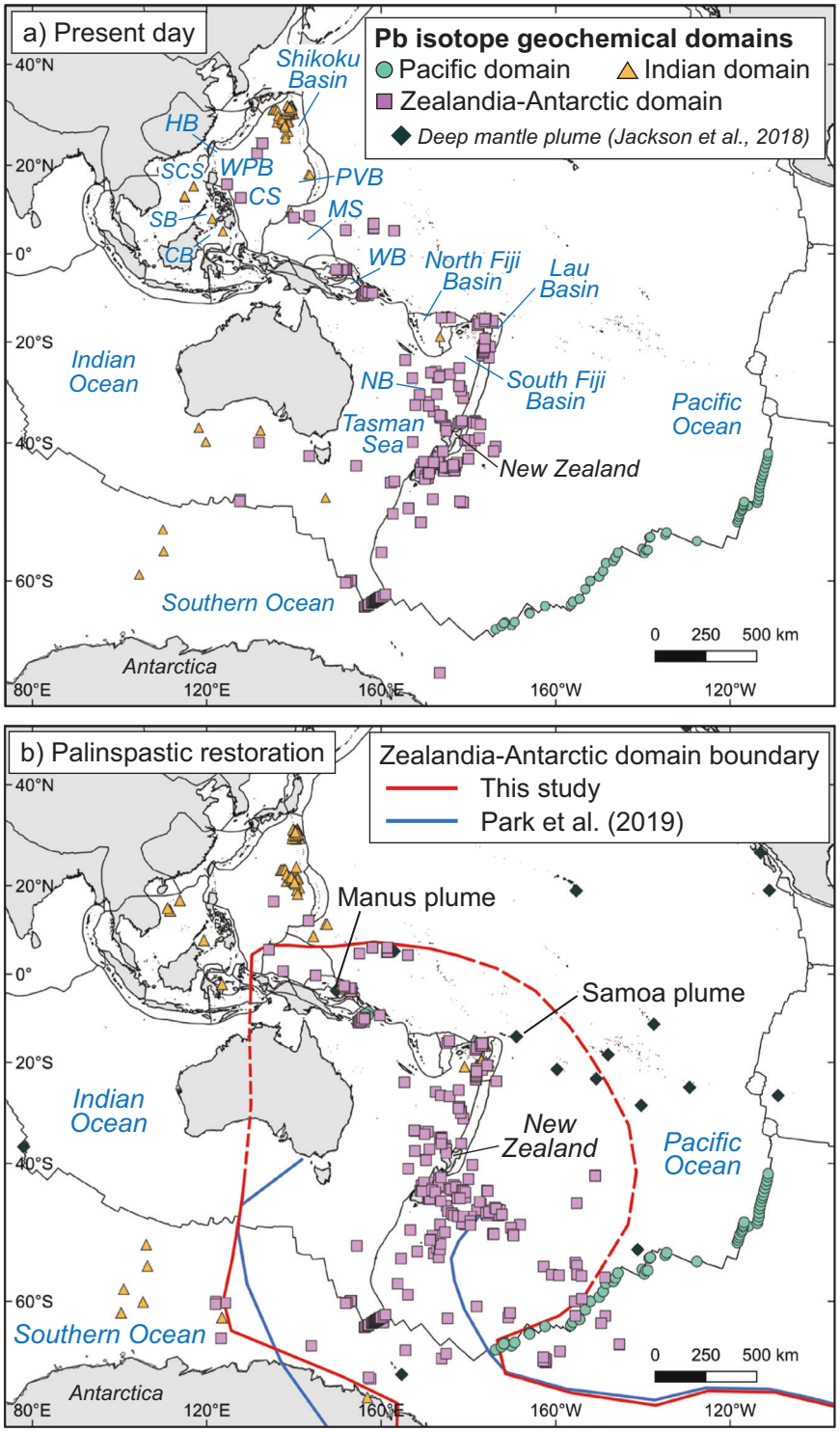

Fig. 7 | Geochemical mantle domain maps showing present-day and palinspastically-restored basalt Pb isotopes from Fig. 5. a Geochemical mantle domains are classified based on the basalts in present locations. **b** The basalts were restored to their original locations using a published plate reconstruction[48]. We newly delineate the Zealandia-Antarctic domain boundary (red line) relative to a previous study[30] (blue line). The red dashed line shows less certain areas of the domain boundary. Filled diamonds are deep mantle plumes[79]. CB: Celebes Basin, CS: Caroline Sea, HB: Huatung Basin, MS: Manus Sea, NB: Norfolk Basin, PVB; Parece-Vela Basin, SB: Sulu basin, SCS: South China Sea, WB: Woodlark Basin, WPB: West Philippine Basin.

of Gagua Ridge lavas were selected for chemical analysis. We conducted an analysis of whole-rock Mo isotopic ratios, which are a promising tracer for geodynamic processes and subduction zone magmatism[63,80]. Our Mo isotopic measurements were taken using a Neptune Plus multi-collector (MC)-ICP-MS at the Guangzhou Institute of Geochemistry, Chinese Academy of Science (GIG-CAS). Chemical separation and mass spectrometry measurements of Mo isotopes were conducted at the State Key Laboratory of Isotope Geochemistry, GIGCAS, following analytical procedures described in ref. 81. Appropriate sample powders were measured to assured 120 ng of Mo and 120 ng of ^{97}Mo-^{100}Mo double spike solution. The Mo double-spike was added before the digestion of bulk rock samples. The samples were digested using 4 mL of HF and 2 mL of HNO_3 in closed beakers at 140 °C overnight. Mo separation and purification were achieved using an extraction chromatographic resin of N-benzoyl-N-phenyl hydroxylamine manufactured in-house following the protocols of ref. 81. After the sample matrix and elements with isobaric interferences were removed, Mo isotope measurement was performed on a Thermo-Fisher Scientific Neptune-Plus multi-collector inductively coupled plasma mass spectrometer (MC–ICP–MS) utilizing double-spike analysis to correct for instrumental mass bias. Isotope measurements are made relative to a NIST SRM 3134 standard solution. The external reproducibility of the NIST SRM 3134 standard solution is 0.06‰ (2 SD, $n = 12$) for the $\delta^{98/95}$Mo values.

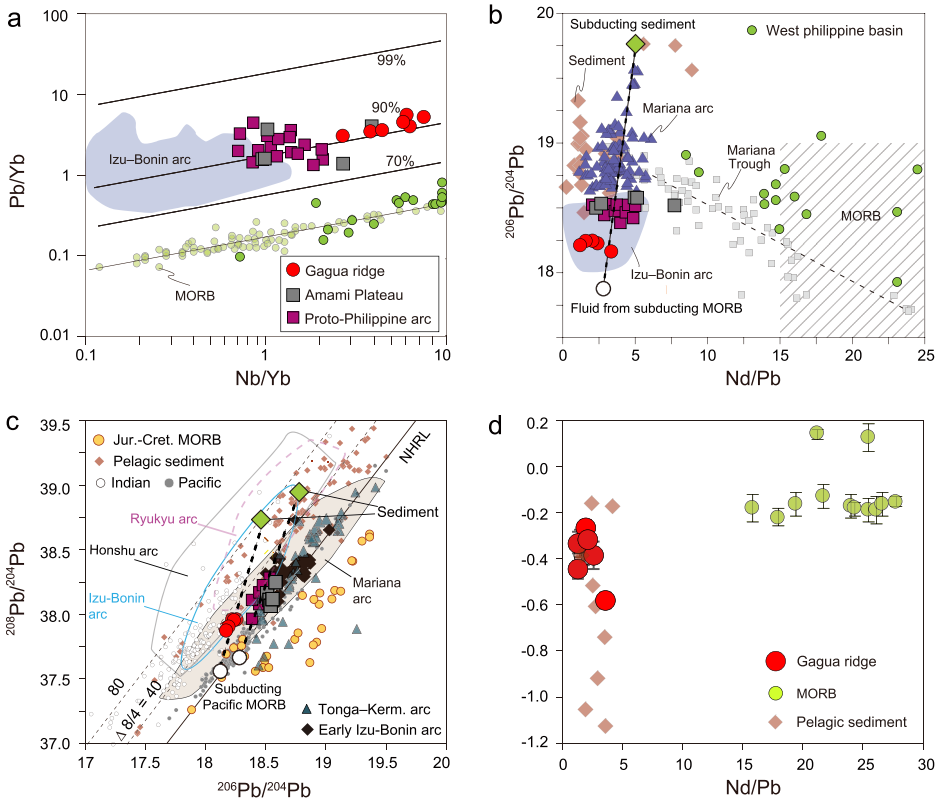

Fig. 8 | Trac element and Pb-Mo isotope systematics. a Pb/Yb vs Nb/Yb for arc lavas and mid-oceanic ridge basalts (MORBs). Trace element ratios of Amami Plateau[36] and proto-Philippine arc[37], Izu Bonin arc lavas[27], and MORBs[85] are shown for comparison. The percentage of subducting slab-derived Pb to the arc is based on a mass balance calculation following Pearce et al.[66]. **b** Nd/Pb versus ^{206}Pb /^{204}Pb. Note the vertical overall trend of the arc magmas. The Mariana arc and Trough volcanics are based on PetDB[95]. **c** Comparisons of initial Pb isotope ratios from other early Cretaceous arc lavas from Amami Plateau and proto-Philippine arc. The trends show the subducting sediment mixing with subducting Pacific MORB (bold dashed lines). Selected volcanic arcs screened for slab input associated with the subduction of Pacific MORB (Tonga–Kermadec) and Indian MORB (Luzon, Honshu, Ryukyu). All arc data are age-corrected. The Indian and Pacific MORB fields are age-corrected to 120 Myr ago, using Th/U = 2.5, and ^{238}U/^{204}Pb = 5. The slab input is not age-corrected. The MORB data are mostly from ref. [94] and references therein, the geochemical data on volcanic arc and sediment were from the GEOROC database[85]. NHRL: Northern Hemisphere Reference Line. **d** Nd/Pb versus δ $^{98/95}$Mo of Gagua ridge lavas. Data sources for arc lava data, sediments, and MORBs as in Figs. 2 and 3.

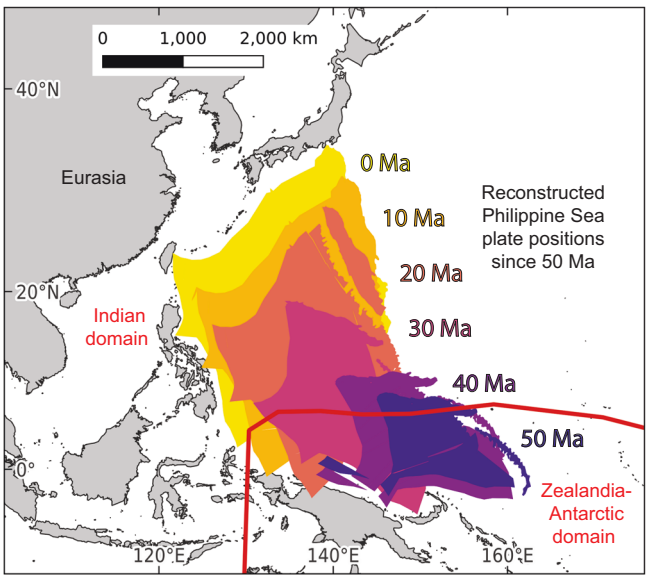

Fig. 9 | Map showing path of Philippine Sea Plate (colored polygons) across the Zealandia-Antarctic domain boundary after 50 Ma. Initially, mid-ocean basalts within the older portion of the plate (i.e., West Philippine Basin) formed by seafloor spreading above the Zealandia-Antarctic domain. Subsequently, the younger, eastern part of the plate (i.e., Shikoku and Parece Vela basins) formed by seafloor spreading above the Indian domain. This sequential development led to the formation of two distinct Pb isotope domains within the Philippine Sea Plate, as shown in Fig. 6.

USGS rock standard BHVO-2 and IAPSO seawater standard were simultaneously processed with each batch of samples to monitor accuracy and gave the δ$^{98/95}$Mo value of −0.04 ± 0.05‰ and 2.06 ± 0.04‰, respectively (Supplementary Data 4). These results are consistent with certified values and with the values reported by previous studies (−0.05 ± 0.11‰ for BHVO and 2.09 ± 0.04‰ for IAPSO)[81,82]. The total procedural blank for our analyses was 0.66 ± 0.37 ng (2 SD, n = 3) Mo, far less than the total Mo in the samples (3.22–6.95 ug/g).

Major and trace element contents of phenocrysts

Major and trace element analyses of clinopyroxene are helpful for understanding petrogenesis and mantle source of Gagua Ridge magma. Major element analyses of clinopyroxene were performed on a JEOL JXA-8230 electron probe micro-analyzer (EPMA) at the SKLMG, Tongji University. The operating conditions for clinopyroxene were a 15 kV accelerating voltage and a 20 nA beam current. A variable peak counting time of 10–120 s was designed for the intensity of the characteristic X-ray lines and desired precision. A range of oxide and silicate (e.g., jadeite, wollastonite) standards (e.g., jadeite for Na, periclase for Mg, wollastonite for Ca, Si, rutile for Ti, fayalite for Fe, K-feldspar for K, corundum for Al, apatite for P, manganotantalite (Mn) and pure metals for Cr, and Ni) were used to calibrate the spectrometers and for matrix reduction of the data.

In-situ trace element analyses of clinopyroxene were carried out by LA-ICP-MS using an excimer 193 nm laser ablation system (GeoLas 2005) in combination with an Agilent 7500 ICP-MS instrument at the GIGCAS. The carrier and make-up gas flows were optimized by ablating NIST SRM 610 to acquire maximum signal intensity for ^{208}Pb, while maintaining low ThO/Th (<0.3%) and Ca^{2+}/Ca^{+} ratios (<0.5%) to reduce interferences of oxides, argides and doubly charged ions as much as possible[83]. The laser parameters were set as following: spot size, 45 μm; repetition rate, 6 Hz; energy density, ~4 J cm^2. Each spot analysis consisted of 30 s gas blank collection with laser off and 50 sample signal collection with laser on. Si content, measured by EPMA, was used for internal standardization. The detailed operating conditions for the laser ablation system and ICP-MS instrument are provided in ref. 83. The analytical precision generally was better than 10% for the standards BCR-2G and BHVO-2G (Supplementary Data 4).

FTIR Analysis of clinopyroxene phenocrysts

The water content (by weight) in the form of structural hydroxy of clinopyroxene phenocrysts is helpful to determine the petrogenesis of

magmatism and was measured by a Bruker VERTEX 80 V Fourier Transform Infrared Spectroscopy instrument coupled with a HYPERION 2000 infrared microscope at the Key Laboratory of Submarine Geoscience, Second Institute of Oceanography, State Oceanic Administration, Hangzhou, China. Double-polished thin sections of rock samples were prepared with thicknesses between 100 and 200 μm. Optically clean, inclusion- and crack-free areas of cpx phenocrysts were chosen for measurement under a continuous dry-air flush. For each cpx analysis, 128 scans with a resolution of 4 cm^{-1} were conducted at wavelengths from 1000 to 5500 cm^{-1} using square apertures (30 × 30 to 100 × 100 μm^2) depending on the grain size and quality. When calculating the water content of cpx, the modified Beer–Lambert law [$c = 3\,A/(I \times t)$] was used, where c, A, I, t represents the water content (wt. ppm), the integrated absorbance of OH bands (cm^{-1}), the molar absorption coefficient (7.09 $ppm^{-1}cm^{-2}$ from ref. 84), and the sample thickness (in cm), respectively.

Geochemical data compilation and spatial reconstruction of western Pacific marginal basin and Southern Ocean lavas

To explore the Indian-Pacific mantle domain boundary, we compiled a comprehensive database of geochemical analyses on volcanic rocks collected within the western Pacific marginal basin and Southern Ocean (Supplementary Data 5). Because the geochemical analyses are collected on mobile tectonic plates, we investigate their implications for locating the Zealandia-Antarctic, Indian, and Pacific mantle domains by palinspastically-restoring the basaltic rocks with published Pb isotopic ratios to their eruption locations. The reconstruction used a global plate reconstruction model and associated mantle reference [48] within the software GPlates and pyGPlates Python library. Plate reconstructions of the western Pacific and Southern Ocean are not fully agreed and we mitigate uncertainty by showing our results within alternative Philippine Sea and East Asian plate reconstructions (Fig. S7)[6,50].

Our analysis requires an assumption that the mantle domains are relatively stable within our reconstruction timeframe. Previous studies indicate the stability of the Indian-Pacific mantle domain since at least ~140 Ma[26]; thus, we compiled geochemical data of Cretaceous to Cenozoic (<130 Ma) basaltic lavas from western Pacific marginal basins and Southern Ocean from Georoc (http://georoc.mpch-mainz.gwdg.de/georoc/)[85]. We minimize potential contamination from continental lithosphere by excluding magmatism within this time window that erupted within continental settings (e.g. eastern Australia). We target basaltic rocks because they are typically produced by partial melting of the mantle; therefore, we only included samples with basaltic affinities (SiO_2 contents less than 55 wt % and $Na_2O + K_2O$ below 10 wt.%). These data that have K_2O/P_2O_5 less than 1 and LOI larger than 5 wt %[86] that indicate alteration were filtered to exclude samples. The volcanic rocks with MgO less than 4 wt % have been excluded because of clinopyroxene, plagioclase, and magnetite fractionation[87]. Some samples appear to be affected by assimilation and fractional crystallization processes and removed as evidenced by the covariations of radiogenic isotopes with indices of differentiation (MgO and SiO_2). In addition, several samples show remarkably low radiogenic isotopes below the bulk of all samples, with $^{143}Nd/^{144}Nd < 0.5121$, and tending toward continental crust signatures. Even though there is no clear indication of contamination, these values have been excluded from our interpretation in a conservative approach to exclude any potential bias.

Data availability

All Supplementary data and Supplementary Movie 1 in this paper are available in the supplementary material and Zenodo dataset: https://doi.org/10.5281/zenodo.10819926.

Received: 9 October 2023; Accepted: 15 March 2024;
Published online: 12 April 2024

References

1. Hall, R. Cenozoic geological and plate tectonic evolution of SE Asia and the SW Pacific: computer-based reconstructions, model and animations. *J. Asian Earth Sci.* **20**, 353–431 (2002).
2. Ishizuka, O., Taylor, R. N., Ohara, Y. & Yuasa, M. Upwelling, rifting, and age-progressive magmatism from the Oki-Daito mantle plume. *Geology* **41**, 1011–1014 (2013).
3. Lallemand, S. Philippine Sea Plate inception, evolution, and consumption with special emphasis on the early stages of Izu-Bonin-Mariana subduction. *Prog. Earth Planet. Sci.* **3**, 15 (2016).
4. Seton, M. et al. Global continental and ocean basin reconstructions since 200. *Ma. Earth-Sci. Rev.* **113**, 212–270 (2012).
5. Taylor, B. & Goodliffe, A. M. The West Philippine Basin and the initiation of subduction, revisited. *Geophys. Res. Lett.* **31**, https://doi.org/10.1029/2004gl020136 (2004).
6. Wu, J., Suppe, J., Lu, R. & Kanda, R. Philippine Sea and East Asian plate tectonics since 52 Ma constrained by new subducted slab reconstruction methods. *J. Geophys. Res.: Solid Earth* **121**, 4670–4741 (2016).
7. Wu, J., Suppe, J., Lu, R. & Kanda, R. Philippine Sea and East Asian plate tectonics since 52 Ma constrained by new subducted slab reconstruction methods. *J. Geophys. Res.: Solid Earth* **121**, 4670–4741 (2016).
8. Xu, J., Ben-Avraham, Z., Kelty, T. & Yu, H.-S. Origin of marginal basins of the NW Pacific and their plate tectonic reconstructions. *Earth-Sci. Rev.* **130**, 154–196 (2014).
9. Hilde, T. W. C. & Lee, C.-S. Origin and evolution of the West Philippine Basin: A new interpretation. *Tectonophysics* **102**, 85–104 (1984).
10. Huang, C.-Y. et al. Potential role of strike-slip faults in opening up the South China Sea. *Natl Sci. Rev.* **6**, 891–901 (2019).
11. Sager, W. W. & Carvallo, C. Paleomagnetism and paleolatitude of igneous drill core samples from the Izu-Bonin forearc and implications for Philippine Sea plate motion. *Tectonophysics* **841**, 229573 (2022).
12. Qian, S. et al. First identification of a Cathaysian continental fragment beneath the Gagua Ridge, Philippine Sea, and its tectonic implications. *Geology* **49**, 1332–1336 (2021).
13. Mrozowski, C. L., Lewis, S. D. & Hayes, D. E. Complexities in the tectonic evolution of the West Philippine Basin. *Tectonophysics* **82**, 1–24 (1982).
14. Deschamps, A. E., Lallemand, S. E. & Collot, J.-Y. A detailed study of the Gagua Ridge: a fracture zone uplifted during a plate reorganisation in the Mid-Eocene. *Mar. Geophys. Res.* **20**, 403–423 (1998).
15. Castillo, P. The Dupal anomaly as a trace of the upwelling lower mantle. *Nature* **336**, 667–670 (1988).
16. Hamelin, B. & Allègre, C. J. Large-scale regional units in the depleted upper mantle revealed by an isotope study of the South-West Indian Ridge. *Nature* **315**, 196–199 (1985).
17. Hanan, B. B., Blichert-Toft, J., Pyle, D. G. & Christie, D. M. Contrasting origins of the upper mantle revealed by hafnium and lead isotopes from the Southeast Indian Ridge. *Nature* **432**, 91–94 (2004).
18. Hart, S. R. A large-scale isotope anomaly in the Southern Hemisphere mantle. *Nature* **309**, 753–757 (1984).
19. Kempton, P. D. et al. Sr-Nd-Pb-Hf isotope results from ODP Leg 187: evidence for mantle dynamics of the Australian-Antarctic discordance and origin of the Indian MORB source. *Geochem. Geophys. Geosyst.* **3**, 1–35 (2002).
20. Klein, E. M., Langmuir, C. H., Zindler, A., Staudigel, H. & Hamelin, B. Isotope evidence of a mantle convection boundary at the Australian-Antarctic Discordance. *Nature* **333**, 623–629 (1988).
21. Vlastélic, I. et al. Large-scale chemical and thermal division of the Pacific mantle. *Nature* **399**, 345–350 (1999).
22. Hofmann, A. W. Mantle geochemistry: the message from oceanic volcanism. *Nature* **385**, 219–229 (1997).
23. Pearce, J. A., Kempton, P. D., Nowell, G. M. & Noble, S. R. Hf-Nd element and isotope perspective on the nature and provenance of

mantle and subduction components in Western Pacific Arc-Basin systems. *J Petrol* **40**, 1579–1611 (1999).
24. Christie, D. M., West, B. P., Pyle, D. G. & Hanan, B. B. Chaotic topography, mantle flow and mantle migration in the Australian–Antarctic discordance. *Nature* **394**, 637–644 (1998).
25. Klein, E. M. & Langmuir, C. H. Global correlations of ocean ridge basalt chemistry with axial depth and crustal thickness. *J. Geophys. Res.: Solid Earth* **92**, 8089–8115 (1987).
26. Miyazaki, T. et al. Missing western half of the Pacific Plate: Geochemical nature of the Izanagi-Pacific Ridge interaction with a stationary boundary between the Indian and Pacific mantles. *Geochem. Geophys. Geosyst.* **16**, 3309–3332 (2015).
27. Straub, S. M., Goldstein, S. L., Class, C. & Schmidt, A. Mid-ocean-ridge basalt of Indian type in the northwest Pacific Ocean basin. *Nat. Geosci.* **2**, 286–289 (2009).
28. Machida, S., Hirano, N. & Kimura, J.-I. Evidence for recycled plate material in Pacific upper mantle unrelated to plumes. *Geochim. Cosmochim. Acta* **73**, 3028–3037 (2009).
29. Nebel, O. et al. Hf–Nd–Pb isotope evidence from Permian arc rocks for the long-term presence of the Indian–Pacific mantle boundary in the SW Pacific. *Earth Planet. Sci. Lett.* **254**, 377–392 (2007).
30. Park, S.-H. et al. An isotopically distinct Zealandia–Antarctic mantle domain in the Southern Ocean. *Nat. Geosci.* **12**, 206–214 (2019).
31. Deschamps, A. & Lallemand, S. The West Philippine Basin: an Eocene to early Oligocene back arc basin opened between two opposed subduction zones. *J. Geophys. Res.* **107**, https://doi.org/10.1029/2001JB001706 (2002).
32. Mrozowski, C. L. & Hayes, D. E. The evolution of the Parece Vela Basin, eastern Philippine Sea. *Earth Planet. Sci. Lett.* **46**, 49–67 (1979).
33. Okino, K., Ohara, Y., Kasuga, S. & Kato, Y. The Philippine Sea: New survey results reveal the structure and the history of the marginal basins. *Geophys. Res. Lett.* **26**, 2287–2290 (1999).
34. Hickey-Vargas, R. Isotope characteristics of submarine lavas from the Philippine Sea: implications for the origin of arc and basin magmas of the Philippine tectonic plate. *Earth Planet. Sci. Lett.* **107**, 290–304 (1991).
35. Hickey-Vargas, R. Origin of the Indian Ocean-type isotopic signature in basalts from Philippine Sea plate spreading centers: An assessment of local versus large-scale processes. *J. Geophys. Res.: Solid Earth* **103**, 20963–20979 (1998).
36. Hickey-Vargas, R. Basalt and tonalite from the Amami Plateau, northern West Philippine Basin: New Early Cretaceous ages and geochemical results, and their petrologic and tectonic implications. *Isl Arc* **14**, 653–665 (2005).
37. Deng, J. et al. Early cretaceous transformation from Pacific to Neo-Tethys subduction in the SW Pacific Ocean: Constraints from Pb-Sr-Nd-Hf isotopes of the Philippine arc. *Geochim. Cosmochim. Acta* **285**, 21–40 (2020).
38. Deschamps, A., Monié, P., Lallemand, S., Hsu, S. K. & Yeh, K. Y. Evidence for Early Cretaceous oceanic crust trapped in the Philippine Sea Plate. *Earth Planet. Sci Lett.* **179**, 503–516 (2000).
39. Queano, K. L., Ali, J. R., Milsom, J., Aitchison, J. C. & Pubellier, M. North Luzon and the Philippine Sea Plate motion model: Insights following paleomagnetic, structural, and age-dating investigations. *J. Geophys. Res.: Solid Earth* **112**, https://doi.org/10.1029/2006jb004506 (2007).
40. Zahirovic, S. et al. Tectonic evolution and deep mantle structure of the eastern Tethys since the latest Jurassic. *Earth-Sci. Rev.* **162**, 293–337 (2016).
41. Eakin, D. H., McIntosh, K. D., Van Avendonk, H. J. A. & Lavier, L. New geophysical constraints on a failed subduction initiation: The structure and potential evolution of the Gagua Ridge and Huatung Basin. *Geochem. Geophys. Geosyst.***16**, 380–400 (2015).
42. Bali, E., Keppler, H. & Audetat, A. The mobility of W and Mo in subduction zone fluids and the Mo–W–Th–U systematics of island arc magmas. *Earth Planet. Sci. Lett.* **351–352**, 195–207 (2012).
43. Skora, S., Freymuth, H., Blundy, J., Elliott, T. & Guillong, M. An experimental study of the behaviour of cerium/molybdenum ratios during subduction: Implications for tracing the slab component in the Lesser Antilles and Mariana Arc. *Geochim. Cosmochim. Acta* **212**, 133–155 (2017).
44. Chen, S. et al. Molybdenum systematics of subducted crust record reactive fluid flow from underlying slab serpentine dehydration. *Nat. Commun.* **10**, 4773 (2019).
45. Freymuth, H., Vils, F., Willbold, M., Taylor, R. N. & Elliott, T. Molybdenum mobility and isotopic fractionation during subduction at the Mariana arc. *Earth Planet. Sci. Lett.* **432**, 176–186 (2015).
46. Roeder, P. L. & Emslie, R. F. Olivine-liquid equilibrium. *Contrib. Min. Petr.* **29**, 275 (1970).
47. O'Leary, J. A., Gaetani, G. A. & Hauri, E. H. The effect of tetrahedral Al3+ on the partitioning of water between clinopyroxene and silicate melt. *Earth Planet. Sci. Lett.* **297**, 111–120 (2010).
48. Muller, R. D. et al. A global plate model including lithospheric deformation along major rifts and Orogens since the Triassic. *Tectonics* **38**, 1884–1907 (2019).
49. Scotese, C. R. & Wright, N. PALEOMAP paleodigital elevation models (PaleoDEMS) for the Phanerozoic. *Paleomap Proj.* https://www.earthbyte.org/paleodem-resource-scotese-and-wright-2018 (2018).
50. Torsvik, T. H. et al. Pacific-Panthalassic reconstructions: Overview, errata and the way forward. *Geochem. Geophys. Geosyst.* **20**, 3659–3689 (2019).
51. Plank, T. & Langmuir, C. H. The chemical composition of subducting sediment and its consequences for the crust and mantle. *Chem. Geol.* **145**, 325–394 (1998).
52. Wallace, P. J. Volatiles in subduction zone magmas: concentrations and fluxes based on melt inclusion and volcanic gas data. *J. Volcanol. Geoth. Res.* **140**, 217–240 (2005).
53. Dixon, J. E., Leist, L., Langmuir, C. & Schilling, J.-G. Recycled dehydrated lithosphere observed in plume-influenced mid-ocean-ridge basalt. *Nature* **420**, 385–389 (2002).
54. Michael, P. Regionally distinctive sources of depleted MORB: Evidence from trace elements and H2O. *Earth Planet. Sci. Lett.* **131**, 301–320 (1995).
55. Ishizuka, O., Taylor, R., Milton, J. A. & Nesbitt, R. Fluid-mantle interaction in an intra-oceanic arc: constraints from high-precision Pb isotopes. *Earth Planet. Sci. Lett.* **211**, 221–236 (2002).
56. Johnson, J. S., Gibson, S. A., Thompson, R. N. & Nowell, G. M. Volcanism in the Vitim Volcanic Field, Siberia: Geochemical evidence for a mantle plume beneath the Baikal Rift zone. *J. Petrol.* **46**, 1309–1344 (2005).
57. Pearce, J. A., Stern, R. J., Bloomer, S. H. & Fryer, P. Geochemical mapping of the Mariana arc-basin system: Implications for the nature and distribution of subduction components. *Geochem. Geophys. Geosyst.* **6**, https://doi.org/10.1029/2004GC000895 (2005).
58. Timm, C. et al. Trench-perpendicular geochemical variation between two adjacent Kermadec Arc Volcanoes Rumble II East and West: the role of the subducted Hikurangi Plateau in element recycling in Arc Magmas. *J. Petrol.* **57**, 1335–1360 (2016).
59. König, S., Wille, M., Voegelin, A. & Schoenberg, R. Molybdenum isotope systematics in subduction zones. *Earth Planet. Sci. Lett.* **447**, 95–102 (2016).
60. Gaschnig, R. M. et al. The molybdenum isotope system as a tracer of slab input in subduction zones: an example from Martinique, lesser Antilles Arc. *Geochem. Geophys. Geosyst.* **18**, 4674–4689 (2017).
61. Wille, M. et al. Molybdenum isotope variations in calc-alkaline lavas from the Banda arc, Indonesia: assessing the effect of crystal fractionation in creating isotopically heavy continental crust. *Chem. Geol.* **485**, 1–13 (2018).
62. McCoy-West, A. J. et al. Extensive crustal extraction in Earth's early history inferred from molybdenum isotopes. *Nat. Geosci.* **12**, 946–951 (2019).

63. Willbold, M. & Elliott, T. Molybdenum isotope variations in magmatic rocks. *Chem. Geol.* **449**, 253–268 (2017).
64. Miller, D., Goldstein, S. & Langmuir, C. Cerium/lead and lead isotope ratios in arc magmas and the enrichment of lead in the continents. *Nature* **368**, 514–520 (1994).
65. Niu, Y. & Batiza, R. Trace element evidence from seamounts for recycled oceanic crust in the Eastern Pacific mantle. *Earth Planet. Sci. Lett.* **148**, 471–483 (1997).
66. Pearce, J. A., Baker, P. E., Harvey, P. K. & Luff, I. W. Geochemical evidence for subduction fluxes, mantle melting and fractional crystallization beneath the South Sandwich Island Arc. *J Petrol* **36**, 1073–1109 (1995).
67. Hickey-Vargas, R., Bizimis, M. & Deschamps, A. Onset of the Indian Ocean isotopic signature in the Philippine Sea Plate: Hf and Pb isotope evidence from Early Cretaceous terranes. *Earth Planet. Sci. Lett.* **268**, 255–267 (2008).
68. Gaina, C. & Müller, D. Cenozoic tectonic and depth/age evolution of the Indonesian gateway and associated back-arc basins. *Earth-Sci. Rev.* **83**, 177–203 (2007).
69. French, S. W. & Romanowicz, B. Broad plumes rooted at the base of the Earth's mantle beneath major hotspots. *Nature* **525**, 95–99 (2015).
70. Courtillot, V., Davaille, A., Besse, J. & Stock, J. Three distinct types of hotspots in the Earth's mantle. *Earth Planet. Sci. Lett.* **205**, 295–308 (2003).
71. Jackson, M. G., Price, A. A., Blichert-Toft, J., Kurz, M. D. & Reinhard, A. A. Geochemistry of lavas from the Caroline hotspot, Micronesia: Evidence for primitive and recycled components in the mantle sources of lavas with moderately elevated 3He/4He. *Chem. Geol.* **455**, 385–400 (2017).
72. O'Connor, J. M. et al. Superplume mantle tracked isotopically the length of Africa from the Indian Ocean to the Red Sea. *Nat. Commun.* **10**, 5493 (2019).
73. Hoernle, K. et al. Late Cretaceous (99-69 Ma) basaltic intraplate volcanism on and around Zealandia: Tracing upper mantle geodynamics from Hikurangi Plateau collision to Gondwana breakup and beyond. *Earth Planet. Sci. Lett.* **529**, 115864 (2020).
74. Hoernle, K. et al. Cenozoic intraplate volcanism on New Zealand: Upwelling induced by lithospheric removal. *Earth Planet. Sci. Lett.* **248**, 350–367 (2006).
75. Timm, C., Hoernle, K., Van Den Bogaard, P., Bindeman, I. & Weaver, S. Geochemical evolution of intraplate volcanism at Banks Peninsula, New Zealand: interaction between asthenospheric and lithospheric melts. *J Petrol* **50**, 989–1023 (2009).
76. Timm, C. et al. Temporal and geochemical evolution of the Cenozoic intraplate volcanism of Zealandia. *Earth-Sci. Rev.* **98**, 38–64 (2010).
77. Yang, A. Y. et al. A subduction influence on ocean ridge basalts outside the Pacific subduction shield. *Nat. Commun.* **12**, 4757 (2021).
78. Doucet, L. S. et al. Distinct formation history for deep-mantle domains reflected in geochemical differences. *Nat. Geosci.* **13**, 511–515 (2020).
79. Jackson, M. G., Becker, T. W. & Konter, J. G. Evidence for a deep mantle source for EM and HIMU domains from integrated geochemical and geophysical constraints. *Earth Planet. Sci. Lett.* **484**, 154–167 (2018).
80. Freymuth, H., Elliott, T., van Soest, M. & Skora, S. Tracing subducted black shales in the Lesser Antilles arc using molybdenum isotope ratios. *Geology* **44**, 987–990 (2016).
81. Li, J. et al. Measurement of the isotopic composition of molybdenum in geological samples by MC-ICP-MS using a novel chromatographic extraction technique. *Geostand. Geoanal. Res.* **38**, 345–354 (2014).
82. Greber, N. D., Siebert, C., Nägler, T. F. & Pettke, T. δ98/95Mo values and molybdenum concentration data for NIST SRM 610, 612 and 3134: towards a common protocol for reporting Mo data. *Geostand. Geoanal. Res.* **36**, 291–300 (2012).
83. Zhang, L. et al. In situ determination of trace elements in melt inclusions using laser ablation inductively coupled plasma sector field mass spectrometry. *Rapid Commun. Mass Spectrom.* **33**, 361–370 (2019).
84. Bell, D. R., Ihinger, P. D. & Rossman, G. R. Quantitative analysis of trace OH in garnet and pyroxenes. *Am. Min.* **80**, 465–474 (1995).
85. GeoROC. Geochemistry of Rocks of the Oceans and Continents. http://georoc.mpch-mainz.gwdg.de/georoc/ (2023).
86. Hofmann, A. in *The Mantle and Core* Vol. 2 (ed. Carlson, R. W.) 61–101 (Sp Elsevier, 2003).
87. Mather, B. R. et al. Intraplate volcanism triggered by bursts in slab flux. *Sci. Adv.* **6**, eabd0953 (2020).
88. Ahmad, Q. et al. The Molybdenum isotope subduction recycling conundrum: a case study from the Tongan subduction zone, Western Alps and Alpine Corsica. *Chem. Geol.* **576**, 120231 (2021).
89. Bezard, R., Fischer-Gödde, M., Hamelin, C., Brennecka, G. A. & Kleine, T. The effects of magmatic processes and crustal recycling on the molybdenum stable isotopic composition of Mid-Ocean Ridge Basalts. *Earth Planet. Sci. Lett.* **453**, 171–181 (2016).
90. Liang, Y.-H. et al. Molybdenum isotope fractionation in the mantle. *Geochim. Cosmochim. Acta* **199**, 91–111 (2017).
91. Workman, R. K. & Hart, S. R. Major and trace element composition of the depleted MORB mantle (DMM). *Earth Planet. Sci. Lett.* **231**, 53–72 (2005).
92. Ruscitto, D. M., Wallace, P. J., Cooper, L. B. & Plank, T. Global variations in H2O/Ce: 2. Relationships to arc magma geochemistry and volatile fluxes. *Geochem. Geophys. Geosyst.* **13**, https://doi.org/10.1029/2011GC003887 (2012).
93. Aizawa, Y., Tatsumi, Y. & Yamada, H. Element transport by dehydration of subducted sediments: Implication for arc and ocean island magmatism. *Isl Arc* **8**, 38–46 (1999).
94. Gale, A., Dalton, C. A., Langmuir, C. H., Su, Y. J. & Schilling, J. G. The mean composition of ocean ridge basalts. *Geochem. Geophys. Geosyst.* **14**, 489–518 (2013).
95. PetDB. Information System for Geochemical Data of Igneous and Metamorphic Rocks from the Ocean Floor. http://www.petdb.org/petdbWeb/index.jsp (2023).

Acknowledgements

The authors are very grateful to Chi-Yue Huang, Huaiyang Zhou, and Matthew G. Jackson for helpful discussions. We thank Lingmin Zhang and Hao Cheng for their assistance in the sample analysis. Stéphane Dominguez is thanked for providing the bathymetric compilation. Shenyang Institute of automation and Zhiguo Qiao are thanked for helping collect the sample. This study was supported by PI Project of Southern Marine Science and Engineering Guangdong Laboratory (Guangzhou) (GML2022006) and the National Natural Science Foundation (NSF) of China (41902044). Jonny Wu and Tsung-Jui Wu were supported by US NSF grant EAR-1848327. We are grateful for comments from three reviewers (Christian Timm and two anonymous reviewers) and Editor Joe Aslin that improved our manuscript.

Author contributions

The geochemical analysis was conducted by S.P.Q. The chemical and isotope data were collected by S.P.Q. and J.T.J.W. The mantle domain reconstruction was conducted by J.T.J.W. The original draft was written by S.P.Q. and J.W. and all authors contributed to the reviewing and editing of this manuscript.

Competing interests

The authors declare no competing interests.

Additional information

Supplementary information The online version contains supplementary material available at https://doi.org/10.1038/s43247-024-01326-6.

Correspondence and requests for materials should be addressed to Shengping Qian or Jonny Wu.

Peer review information *Communications Earth & Environment* thanks Dietmar Muller, Christian Timm and the other, anonymous, reviewer(s) for their contribution to the peer review of this work. Primary Handling Editor: Joe Aslin. A peer review file is available.